Motor Control Application

Sensorless Vector Control for Permanent Magnet Synchronous Motor (Algorithm)

Summary

This application note explains the speed control algorithm in the sensorless vector control software for permanent magnet synchronous motor (PMSM) using Renesas Electronics Corporation's microcontroller.

Contents

1. Overview

This application note explains the speed control algorithm in the sensorless vector control software for permanent magnetic synchronous motor (PMSM) using Renesas Electronics Corporation's microcontroller.

2. PMSM Fundamental Equation

2.1   PMSM Model in Three-Phase (U, V, W) Coordinate

Voltage equation of the permanent magnet synchronous motor having sinusoidal magnetic flux distribution (Figure 2-1) can be expressed as follows.
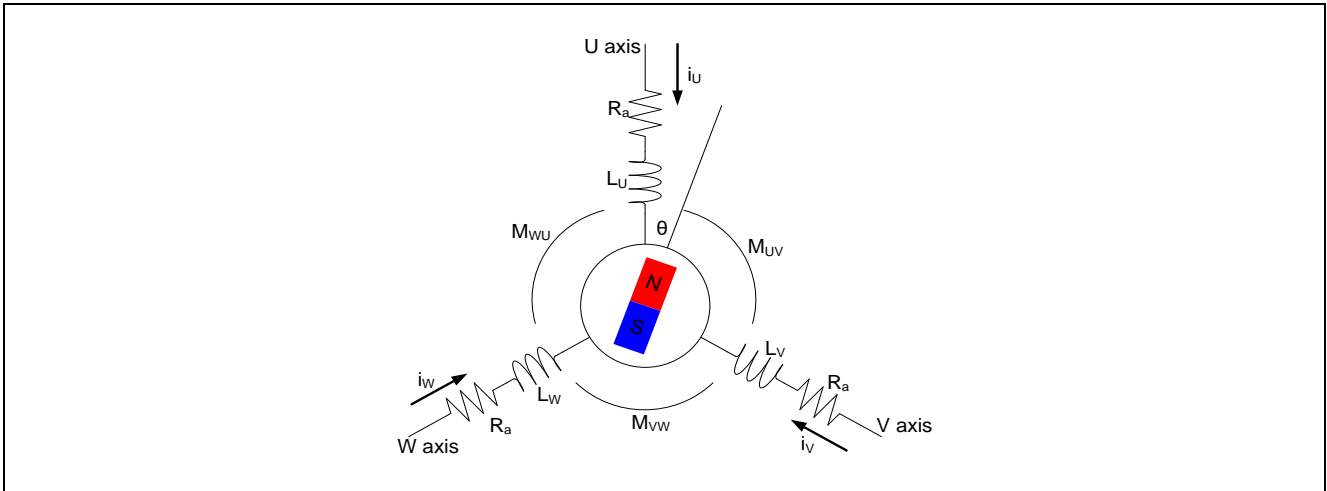

Figure 2-1 Conceptual Diagram of Three-Phase Permanent Magnet Synchronous Motor

$$\begin{bmatrix} v_u \\ v_v \\ v_w \end{bmatrix} = R_a \begin{bmatrix} i_u \\ i_v \\ i_w \end{bmatrix} + p \begin{bmatrix} \phi_u \\ \phi_v \\ \phi_w \end{bmatrix}$$

$$\begin{bmatrix} \phi_u \\ \phi_v \\ \phi_w \end{bmatrix} = \begin{bmatrix} L_u & M_{uv} & M_{wu} \\ M_{uv} & L_v & M_{vw} \\ M_{wu} & M_{vw} & L_w \end{bmatrix} \begin{bmatrix} i_u \\ i_v \\ i_w \end{bmatrix} + \psi \begin{bmatrix} cos\theta \\ \cos(\theta - 2\pi/3) \\ \cos(\theta + 2\pi/3) \end{bmatrix}$$

v_u, v_v, v_w : Stator phase voltage L_u, L_v, L_w : Stator phase self-inductance

i_u, i_v, i_w : Stator phase current M_{uv}, M_{vw}, M_{wu} : Mutual inductance

ϕ_u, ϕ_v, ϕ_w : Stator phase interlinkage flux ψ : Maximum flux linkage due to permanent magnet

R_a : Stator phase resistance θ : Rotor electrical angle from phase U

p : Differential operator

2.2 PMSM Model in Direct-Quadrature (d, q) Coordinate

Vector control is a method to control the motor on the two-phase (d, q) coordinate system instead of the three-phase (u,v,w) coordinate system.

The d-axis is set in the direction of the magnetic flux (N pole) of the permanent magnet and the q-axis is set in the direction which progresses by 90 degrees (electrical) in the forward direction of the angle θ from the d-axis.
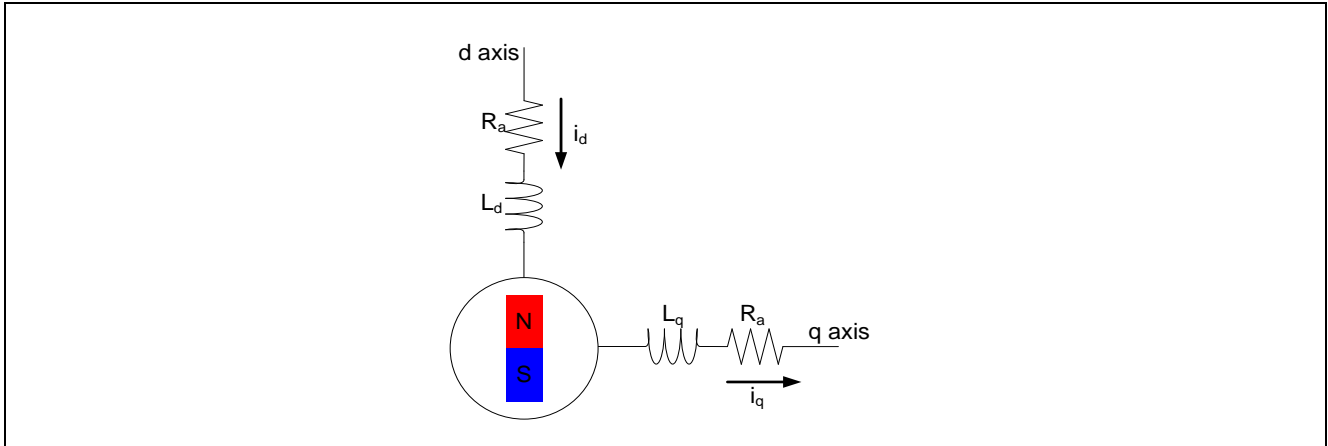

Figure 2-2 Conceptual Diagram of the Two-Phase Direct Current Motor

The coordinate transformation is performed by the following transformation matrix.

$$C = \sqrt{\frac{2}{3}} \begin{bmatrix} cos\theta & \cos(\theta - 2\pi/3) & \cos(\theta + 2\pi/3) \\ -sin\theta & -\sin(\theta - 2\pi/3) & -\sin(\theta + 2\pi/3) \end{bmatrix}$$

$$\begin{bmatrix} v_d \\ v_q \end{bmatrix} = C \begin{bmatrix} v_u \\ v_v \\ v_w \end{bmatrix}$$

The voltage equation in the two-phase (d, q) coordinate system is obtained as follows.

$$\begin{bmatrix} v_d \\ v_q \end{bmatrix} = \begin{bmatrix} R_a + pL_d & -\omega L_q \\ \omega L_d & R_a + pL_q \end{bmatrix} \begin{bmatrix} i_d \\ i_q \end{bmatrix} + \begin{bmatrix} 0 \\ \omega\psi_a \end{bmatrix}$$

v_d, v_q : d-axis and q-axis voltage

i_d, i_q : d-axis and q-axis current

R_a : Stator phase resistance

ω : Angular speed

L_d, L_q : d-axis and q-axis inductance

$L_d = l_a + \dfrac{3(L_a - L_{as})}{2}, L_q = l_a + \dfrac{3(L_a + L_{as})}{2}$

ψ_a : Flux linkage due to permanent magnet

$\psi_a = \sqrt{\dfrac{3}{2}}\psi$

Based on this, it can be considered that alternate current flowing in the stationary three-phase stator is equivalent to direct current flowing in the two-phase stator rotating synchronously with the permanent magnet operating as a rotor.

The generated torque can be written as follows from the exterior product of the electric current vector and armature inter-linkage magnetic flux. The first term on the right side of this formula is called magnet torque and the second term on the right side of this formula is called reluctance torque.

$$T = P_n\{\psi_a i_q + (L_d - L_q)i_d i_q\}$$

T : Motor torque P_n : Number of pole pairs

The PMSM which has no difference between the d-axis and q-axis inductances is defined as non-salient PMSM. In this case, as the reluctance torque is 0, the total torque is proportional to the q-axis current. Due to this, the q-axis current is called torque current. In two-phase (d, q) phase coordinate, the d-axis flux is sum of permanent magnet flux and flux generated by d-axis current. Since the equivalent rotating stator flux (in three-phase (u, v, w) coordinate system) is controlled by d-axis current, the d-axis current is called as excitation current

3.   Control System Design

3.1   Vector Control System and the Controller

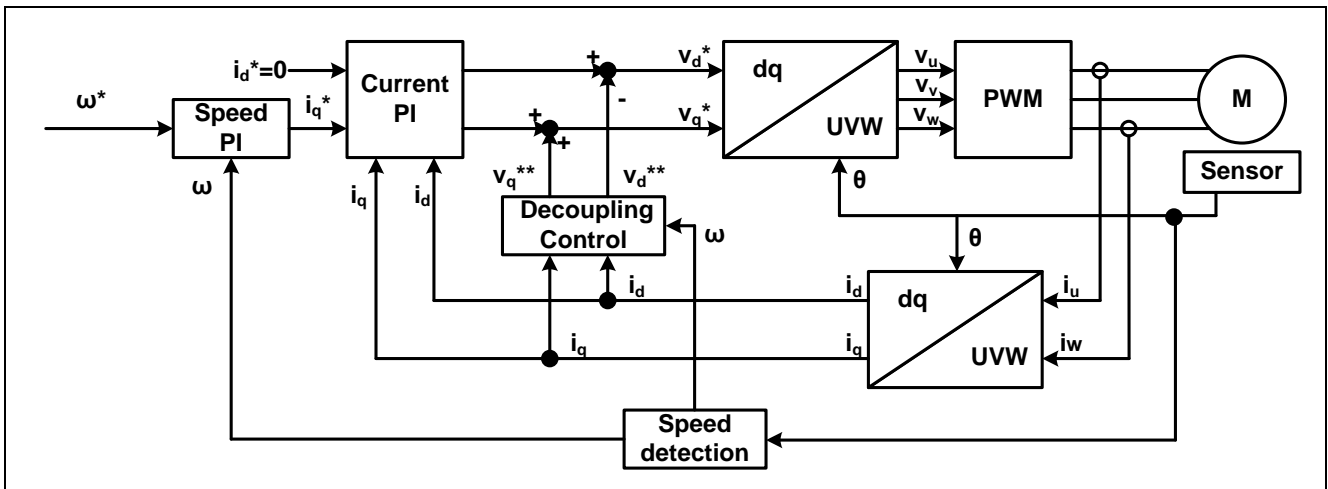Speed control block diagram of the vector control is shown below.

Figure 3-1 Vector Control System Block (Speed Control)

As shown in Figure 3-1, this system consists of the speed control system and the current control system. These systems use general PI controller. PI controller gains of each system must be designed properly to realize required control characteristics.

In decoupling control block, v_d^{**}, v_q^{**} (as the following equations) are calculated and then added to voltage command value. This realizes the high response of speed control system and enables to control the d-axis and q-axis independently.

$$v_d^{**} = -\omega L_q i_q$$

$$v_q^{**} = \omega(L_d i_d + \psi_a)$$

3.2   Current Control System

3.2.1   Design of Current Control System

The current control system is modeled by using the electrical characteristics of the motor. The stator coil can be represented by a resistance R and an inductance L. The stator model of the motor is expressed by the transfer function of the typical RL series circuit $\frac{1}{R+Ls}$.

The current control system model can be represented by a feedback control system using PI control. (Figure 3-2)

R: Resistance of stator coils [Ω] L: Inductance of stator coils [H]

K_p: Proportional gain of the current PI control K_i: Integral gain of the current PI control
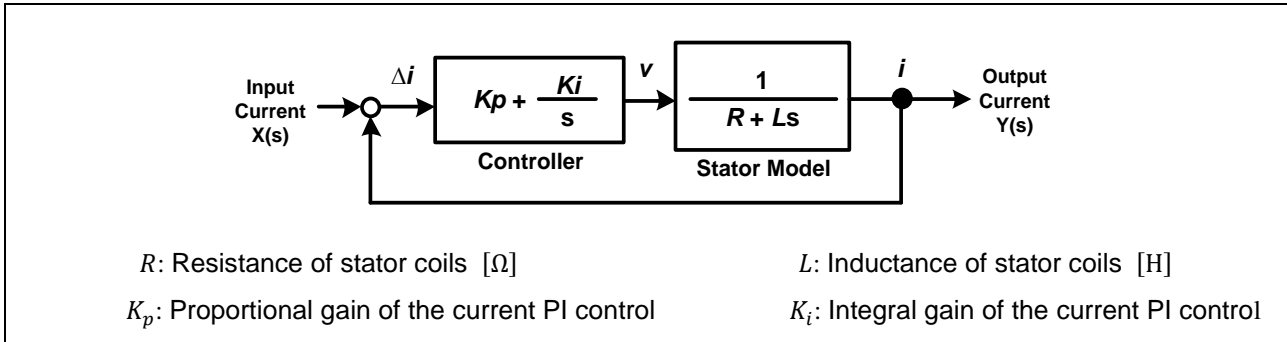
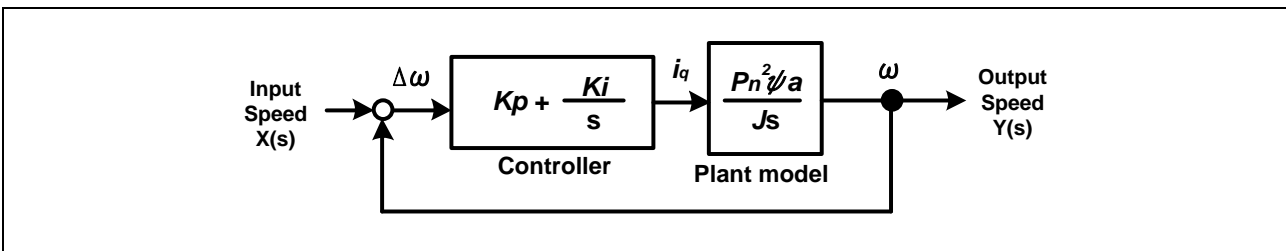**Figure 3-2 Current Control System Model**

Based on this model, PI gains of the current control system are designed as the following method.

First, the closed-loop transfer function of this system is obtained as follows.

$$G(s) = \frac{Y(s)}{X(s)} = \frac{\dfrac{K_a}{K_b}\left(1 + \dfrac{s}{a}\right)}{s^2 + \dfrac{1}{K_b}\left(1 + \dfrac{K_a}{a}\right)s + \dfrac{K_a}{K_b}}$$

$$K_i = K_p a, \qquad K_a = \frac{K_p a}{R}, \qquad K_b = \frac{L}{R}$$

The general equation of second-order lag system with zero point can be expressed as follows.

$$\frac{\omega_n^2}{s^2 + 2\zeta\omega_n s + \omega_n^2}\left(1 + \frac{s}{\omega_z}\right)$$

By comparing coefficients of two equations above, the following equations are obtained.

$$\frac{\omega_n^2\left(1+\frac{s}{\omega_z}\right)}{s^2+2\zeta\omega_n s+\omega_n^2} \Leftrightarrow \frac{\frac{K_a}{K_b}*\left(1+\frac{s}{a}\right)}{s^2+\frac{1}{K_b}(1+\frac{K_a}{a})s+\frac{K_a}{K_b}}$$

$$\omega_n^2=\frac{K_a}{K_b}, \qquad 2\zeta\omega_n=\frac{1}{K_b}\left(1+\frac{K_a}{a}\right), \qquad \omega_z=a$$

From above equations, natural frequency ω_n, damping ratio ζ, zero-point frequency ω_z are written as follows.

$$\omega_n=\sqrt{\frac{K_a}{K_b}}, \qquad \zeta=\frac{1}{2K_b\sqrt{\frac{K_a}{K_b}}}(1+\frac{K_a}{a}), \qquad \omega_z=a=\frac{\omega_n^2 L}{2\zeta\omega_n L-R}$$

Current PI control gains ($K_{p\_current}$,$K_{i\_current}$) are written as the following equations.

$$K_{p\_current}=2\zeta_{CG}\omega_{CG}L-R, \qquad K_{i\_current}=K_{p\_current}a=\omega_{CG}^2 L$$

ω_{CG}: Desired natural frequency of current control system

ζ_{CG}: Desired damping ratio of current control system

Therefore, PI control gains of the current control system can be designed by ω_{CG} and ζ_{CG}.

3.3   Speed Control System

3.3.1   Design of Speed Control System

The speed control system is modeled by using the mechanical characteristics of the motor. The mechanical system torque equation is written as follows.

$$T = J\dot{\omega}_{mech}$$

J: Inertia of rotor, ω_{mech}: Speed (Mechanical)

In consideration of only magnet torque, the electrical system torque equation is written as follows.

$$T = P_n \psi_a i_q$$

By using the mechanical and electrical torque equation, the speed (mechanical) is written as follows.

$$\omega_{mech} = \frac{P_n \psi_a}{sJ} i_q$$

The speed in the control software is treated as the electrical speed. Thereby, the number of pole pairs P_n is multiplied to both sides of this equation.

$$\omega_{elec} = \frac{P_n{}^2 \psi_a}{sJ} i_q$$

ω_{elec}: Speed (Electrical)

The speed control system model can be represented by a feedback control system using PI control. (Figure 3-3)

Figure 3-3 Speed Control System Model

Based on this model, PI gains of the speed control system are designed as the following method.

First, the closed-loop transfer function of this system is obtained as follows.

$$G(s) = \frac{Y(s)}{X(s)} = \frac{K_b \left(1 + \frac{s}{a}\right)}{s^2 + K_b s + K_b a}$$

$$K_b = \frac{K_P P_n^2 \psi_a}{J} \qquad K_i = K_p a$$

The general equation of second-order lag system with zero point can be expressed as follows.

$$\frac{\omega_n^2}{s^2 + 2\zeta\omega_n s + \omega_n^2} \left(1 + \frac{s}{\omega_z}\right)$$

Similar to the current control system, by comparing coefficients of two equations above, the following equations are obtained.

$$\frac{\omega_n^2(1 + s/\omega_z)}{s^2 + 2\zeta\omega_n s + \omega_n^2} \Leftrightarrow \frac{aK_b \left(1 + \frac{s}{a}\right)}{s^2 + K_b s + aK_b}$$

$$\omega_n^2 = aK_b = \frac{K_p a P_n^2 \psi_a}{J}, \qquad 2\zeta\omega_n = K_b = \frac{K_p P_n^2 \psi_a}{J}, \qquad \omega_z = a$$

From above equations, natural frequency ω_n, damping ratio ζ, zero-point frequency ω_z are written as follows.

$$\omega_n = \sqrt{\frac{K_p a P_n^2 \psi_a}{J}}, \qquad \zeta = \frac{1}{2}\sqrt{\frac{K_p P_n^2 \psi_a}{aJ}}, \qquad \omega_z = a = \frac{\omega_n}{2\zeta}$$

Speed PI control gains (K_{p_speed}, K_{i_speed}) are written as the following equations.

$$K_{p\_speed} = \frac{2\zeta_{SG}\omega_{SG}J}{P_n^2 \psi_a}, \qquad K_{i\_speed} = K_{p\_speed} a = \frac{\omega_{SG}^2 J}{P_n^2 \psi_a}$$

ω_{SG}: Desired natural frequency of speed control system

ζ_{SG}: Desired damping ratio of speed control system

Therefore, PI control gains of the speed control system can be designed by ω_{SG} and ζ_{SG}.

4. Sensorless Vector Control

4.1 Position/Speed Estimation Method Based on The BEMF Observer

When the position sensors are not used, in other words, in the case of the sensorless vector control, it is necessary to estimate the position by some methods. These days, the demand for sensorless motor control has increased and several methods are provided for estimating the position. This part introduces the sensorless vector control, which is using the BEMF observer.
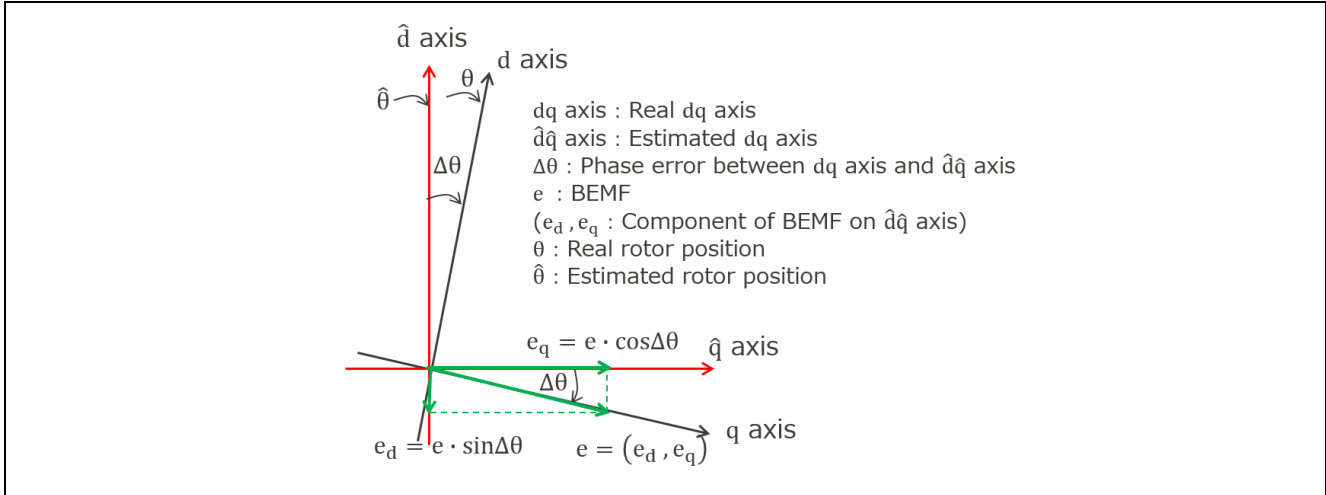
Figure 4-1 BEMF on The Estimated dq Axis

According to Figure 4-1, the voltage equation on the estimated dq axis is written as follows.

$$v_d^* = (R + sL_d)i_d - \omega^* L_q i_q + e_d$$
$$v_q^* = (R + sL_q)i_q + \omega^* L_d i_d + e_q$$

Furthermore, by considering $-\omega^* L_q i_q + e_d$ and $\omega^* L_d i_d + e_q$ as the voltage disturbance, they are written as $-d_d, -d_q$ respectively.

$$v_d^* = (R + sL_d)i_d - d_d$$
$$v_q^* = (R + sL_q)i_q - d_q$$

d-axis voltage equation is rewritten as follows.

$$si_d = \frac{v_d^*}{L_d} - \frac{R}{L_d}i_d + \frac{d_d}{L_d}$$

According to the above equation, state equation is written as follows. The state variables are the d-axis current and the voltage disturbance.

$$si_d = -\frac{R}{L_d}i_d + \frac{d}{L_d} + \frac{v_d^*}{L_d}$$
$$sd = sd_d$$

If the estimated i_d is $\hat{\iota_d}$ and the estimated d is $\hat{d}$, the estimated state equation is written as follows. K_{Ed1} and K_{Ed2} are estimation gains.

$$s\hat{\iota_d} = -\frac{R}{L_d}\hat{\iota_d} + \frac{\hat{d}}{L_d} + \frac{v_d^*}{L_d} + K_{Ed1}(i_d - \hat{\iota_d})$$
$$s\hat{d} = K_{Ed2}(i_d - \hat{\iota_d})$$

According to the above equations, $\hat{\iota_d}$ and $\hat{d}$ are written as follows.

$$\hat{\iota_d} = \frac{\frac{K_{Ed2}}{L_d}}{s^2 + \left(\frac{R}{L_d} + K_{Ed1}\right)s + \frac{K_{Ed2}}{L_d}}\left\{\left(1 + \frac{K_{Ed1}}{K_{Ed2}}L_d s\right)i_d + \frac{s}{K_{Ed2}}v_d^*\right\}$$

$$\hat{d} = \widehat{d_d} = \frac{\frac{K_{Ed2}}{L_d}}{s^2 + \left(\frac{R}{L_d} + K_{Ed1}\right)s + \frac{K_{Ed2}}{L_d}}\{(L_d s + R)i_d - v_d^*\}$$

As shown in the above equations, $\hat{\iota_d}$ and $\widehat{d_d}$ are the 2nd order lag system with input i_d and v_d^*.

Natural frequency ω_n, damping ratio ζ are written as follows.

$$\omega_n = \sqrt{\frac{K_{Ed2}}{L_d}}$$

$$\zeta = \frac{\frac{R}{L_d} + K_{Ed1}}{2\sqrt{\frac{K_{Ed2}}{L_d}}}$$

The characteristic of the estimation system is designed by ω_n and ζ.

The estimation gains are written as follows.

$$K_{Ed1} = 2\zeta_{EG}\omega_{EG} - \frac{R}{L_d}$$

$$K_{Ed2} = \omega_{EG}^2 L_d$$

ω_{EG}: Desired natural frequency of BEMF estimation system

ζ_{EG}: Desired damping ratio of BEMF estimation system

Furthermore, the estimated state equation is rewritten as follows.

$$\widehat{\iota_d} = \frac{1}{s}\left\{-\frac{R}{L_d}\widehat{\iota_d} + \frac{\widehat{d_d}}{L_d} + \frac{v_d^*}{L_d} + K_{Ed1}(i_d - \widehat{\iota_d})\right\}$$

$$\widehat{d_d} = \frac{1}{s}\{K_{Ed2}(i_d - \widehat{\iota_d})\}$$

According to the above equations, the block diagram of the BEMF observer on d-axis can be drew as shown in Figure 4-2.
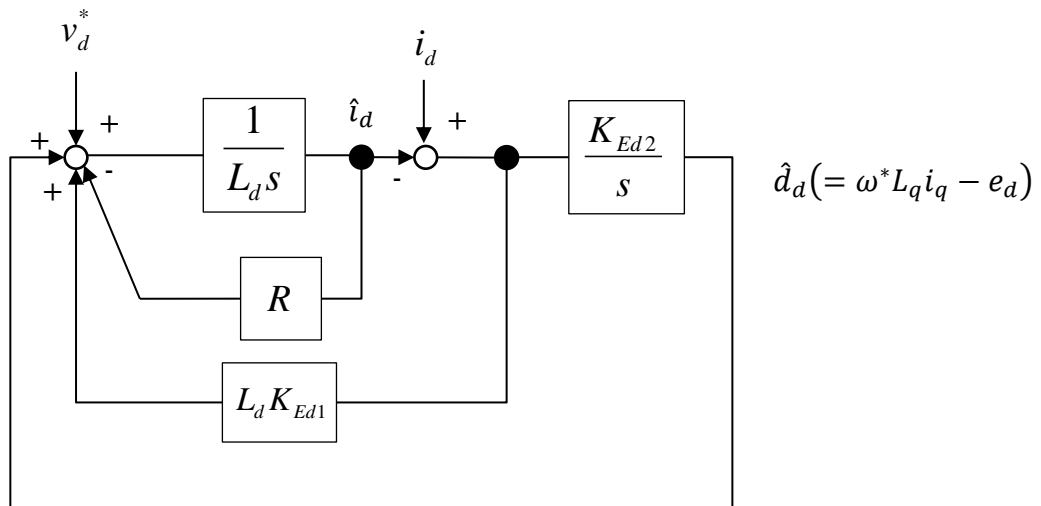
Figure 4-2 Block Diagram of the BEMF Observer on d-Axis

The same calculation can be also realized on q-axis.

$\widehat{\iota_q}$ and $\hat{d}$ are written as follows.

$$\widehat{\iota_q} = \frac{\dfrac{K_{Eq2}}{L_q}}{s^2 + \left(\dfrac{R}{L_q} + K_{Eq1}\right)s + \dfrac{K_{Eq2}}{L_q}} \left\{\left(1 + \frac{K_{Eq1}}{K_{Eq2}}L_q s\right)i_q + \frac{s}{K_{Eq2}}v_q^*\right\}$$

$$\hat{d} = \widehat{d_q} = \frac{\dfrac{K_{Eq2}}{L_q}}{s^2 + \left(\dfrac{R}{L_q} + K_{Eq1}\right)s + \dfrac{K_{Eq2}}{L_q}} \left\{(L_q s + R)i_q - v_q^*\right\}$$

As shown in the above equations, $\widehat{\iota_q}$ and $\widehat{d_q}$ are the 2nd order lag system with input i_q and v_q^*.

Natural frequency ω_n, damping ratio ζ are written as follows.

$$\omega_n = \sqrt{\frac{K_{Eq2}}{L_q}}$$

$$\zeta = \frac{\dfrac{R}{L_q} + K_{Eq1}}{2\sqrt{\dfrac{K_{Eq2}}{L_q}}}$$

The characteristic of the estimation system is designed by ω_n and ζ.
The estimation gains are written as follows.

$$K_{Eq1} = 2\zeta_{EG}\omega_{EG} - \frac{R}{L_q}$$

$$K_{Eq2} = \omega_{EG}^2 L_q$$

ω_{EG}: Desired natural frequency of BEMF estimation system

ζ_{EG}: Desired damping ratio of BEMF estimation system

Furthermore, the estimated state equation is rewritten as follows.

$$\widehat{\iota_q} = \frac{1}{s}\left\{ -\frac{R}{L_q}\widehat{\iota_q} + \frac{\widehat{d_q}}{L_q} + \frac{v_q^*}{L_q} + K_{Eq1}\left(i_q - \widehat{\iota_q}\right)\right\}$$

$$\widehat{d_q} = \frac{1}{s}\left\{K_{Eq2}\left(i_q - \widehat{\iota_q}\right)\right\}$$

According to the above equations, the block diagram of the BEMF observer on q-axis is shown in Figure 4-3.
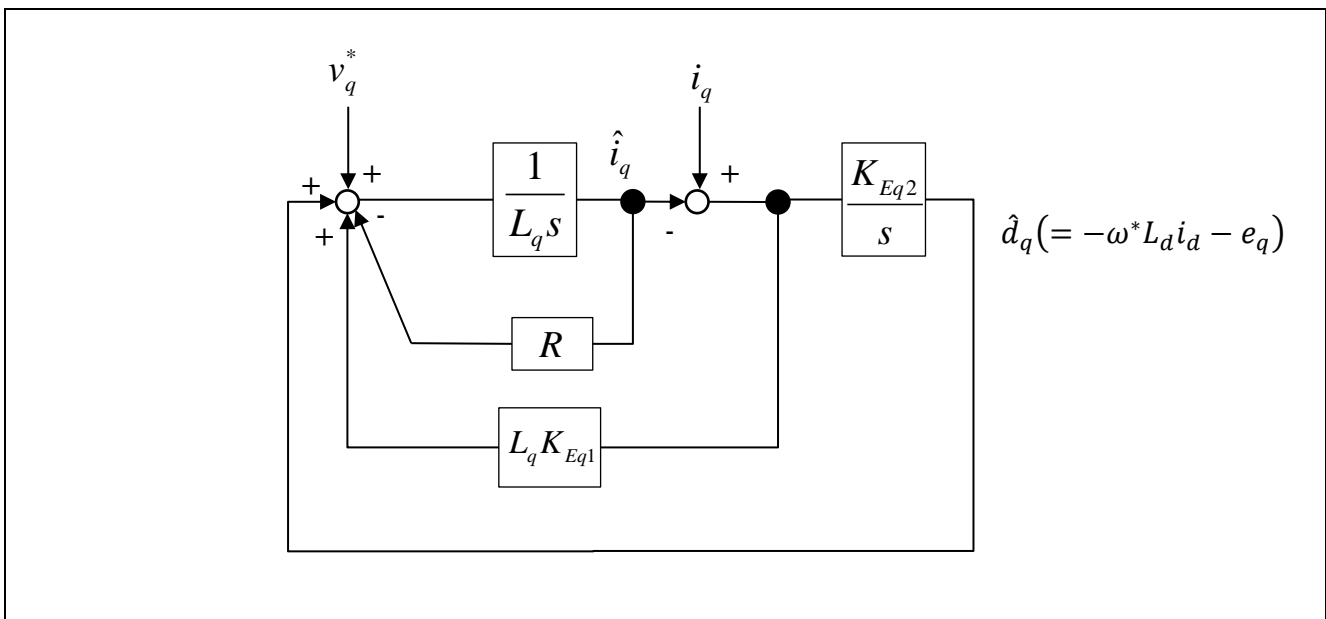
Figure 4-3 Block Diagram of the BEMF Observer on q-Axis

Next, BEMF is calculated from the estimated voltage disturbance $\widehat{d_d}$, $\widehat{d_q}$ as follows.

$$e_d = -\widehat{d_d} + \omega^* L_q i_q$$

$$e_q = -\widehat{d_q} - \omega^* L_d i_d$$

$$\Delta\theta = \mathrm{atan}\left(\frac{e_d}{e_q}\right)$$

As shown in the above equations, the phase error between the real axis and the estimated axis are calculated.

Finally, $\Delta\theta$ is used to estimate rotor position by the method shown in Figure 4-4.
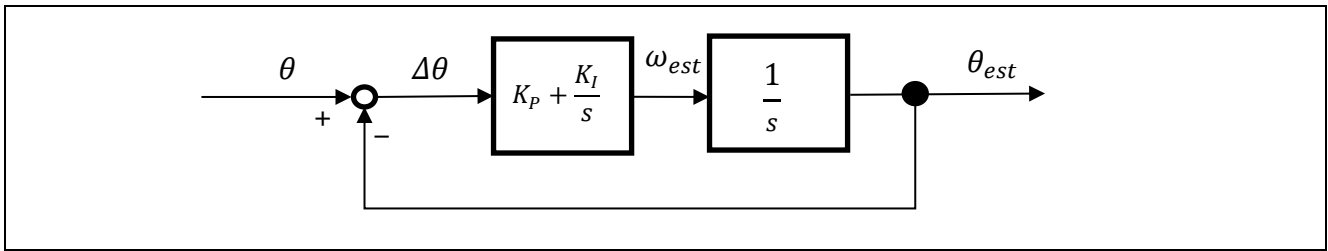
Figure 4-4 Block Diagram of the Position Estimation System

According to the above block diagram, the closed-loop transfer function of this system is

$$\frac{\theta_{est}(s)}{\theta(s)} = \frac{K_I\left(s\frac{K_P}{K_I} + 1\right)}{s^2 + K_P s + K_I}$$

This system is a 2nd order lag system. The natural frequency ω_n, damping ratio ζ are written as follows.

$$\omega_n = \sqrt{K_I}$$

$$\zeta = \frac{K_P}{2\sqrt{K_I}}$$

The control gains of this system ($K_{P\_phase\_error}$, $K_{I\_phase\_error}$) are written as follows.

$$K_{P\_phase\_error} = 2\zeta_{\Delta\theta}\,\omega_{\Delta\theta}$$

$$K_{I\_phase\_error} = \omega_{\Delta\theta}^2$$

$\omega_{\Delta\theta}$: Desired natural frequency of position estimation system

$\zeta_{\Delta\theta}$: Desired damping ratio of position estimation system

As above, the rotor position/speed estimation is completed.

4.2   Open-Loop Control

In the conventional sensorless vector control, the position/speed estimation error in low-speed region is not negligible. Accordingly, in the low-speed region, the motor runs with open-loop control. In this case, motor speed vibrates with natural frequency (depends on current and motor parameters). Figure 4-5 shows the block diagram of the open-loop damping control. This reduces vibration of the motor and realizes stable motor speed.

e_d: Estimated d-axis BEMF (output of the BEMF observer) [V]

Δe_d: Vibration component of estimated d-axis BEMF [V]

K_{damp}: Feedback gain

ω_{comp}: Feedback speed [rad/s (Electrical)]
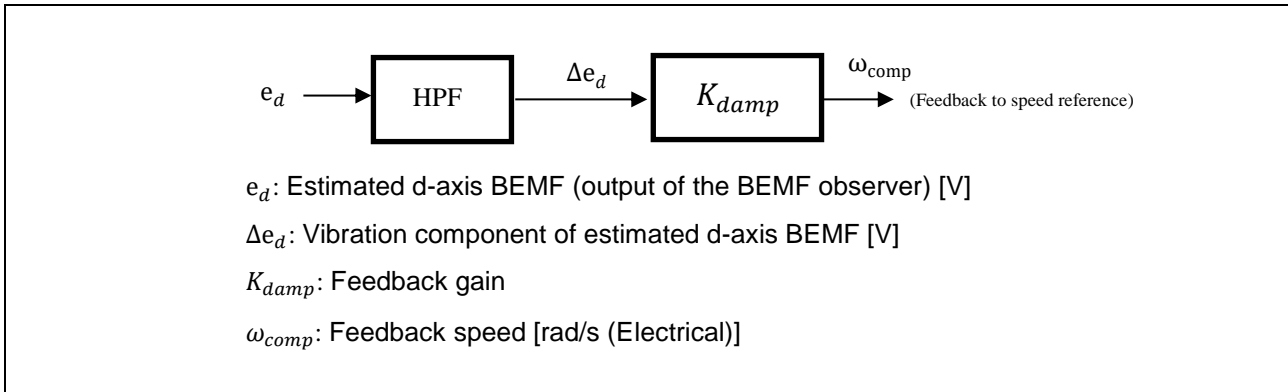
Figure 4-5 Block Diagram of the Open-Loop Damping Control

When the motor speed reaches the region that position/speed estimation error is negligible, the control mode is shifted from open-loop control to sensorless control (closed loop control). But in the open-loop control, especially when the load is heavy, the phase error is large. In this case, shock in current and speed is caused at the control transition timing. Therefore, we use the phase error $\Delta\theta$ to calculate the torque current required to set the phase error to 0 at the control transition, and implement the processing to reflect the calculated torque current to the q-axis current reference (Sensorless transition control) as shown in Figure 4-6. This makes it possible to reduce shock in current and speed at the control transition.
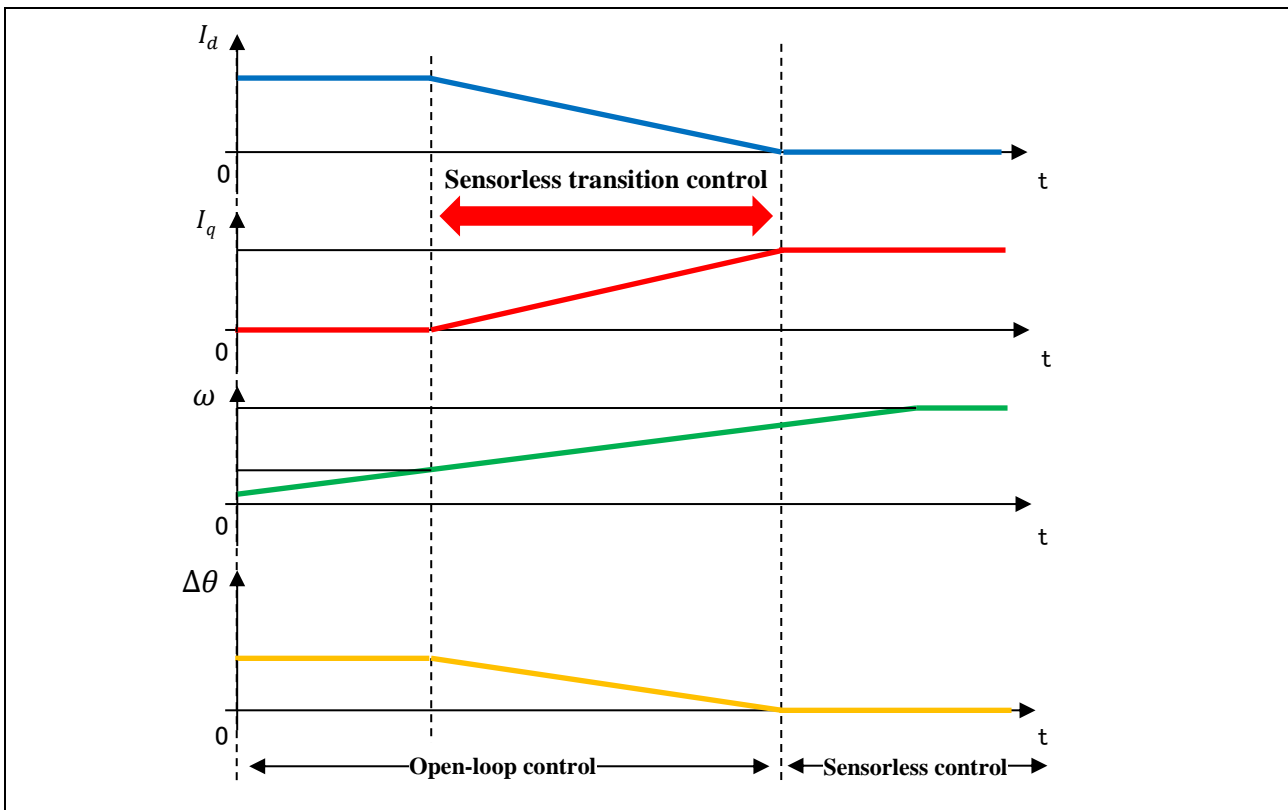
Figure 4-6 Sequence of Sensorless Transition Control

4.3 Flux-weakening Control

BEMF of a PMSM is proportional to the magnetic flux of the rotor and the rotation speed. Then, when the rotation speed increases and BEMF is equal to the power supply voltage, that is, when the voltage saturates, no more current can be passed to the motor, and the rotation speed saturates. It is difficult to achieve both high torque and high speed rotation of a PMSM. For example, a PMSM equipped with a strong magnet increases the torque, but BEMF also increases. In this case, high-speed rotation cannot be realized. Flux-weakening control is a technique to solve this problem.

In the flux-weakening control, applying negative d-axis current prevents voltage saturation due to the BEMF. This achieves high-speed rotation and improves torque output in the high-speed region.

In the software implementation, the d-axis current is determined according to the following formula.

$$I_d = \frac{-\psi_a + \sqrt{\left(\frac{V_{om}}{\omega}\right)^2 - \left(L_q I_q\right)^2}}{L_d}$$

$$\because V_{om} = V_{amax} - I_a R$$

V_{om}: Limit of BEMF [V]

V_{amax}: Maximum value of magnitude of voltage vector [V]

I_a: Magnitude of current vector [A]

4.4   Voltage Error Compensation

The 3-phase inverter has deadtime to prevent short circuit between upper and lower arm of switching devices. Therefore, the voltage reference and the voltage applied the motor have error. This error causes degradation of control accuracy. The voltage error compensation is implemented to reduce this error.

The voltage error depends on the current (direction and magnitude), the deadtime and the switching device characteristic. The voltage error dependence on phase current is shown in Figure 4-7. The voltage error compensation can be realized by adding the voltage, opposite to the voltage error, to the voltage reference.
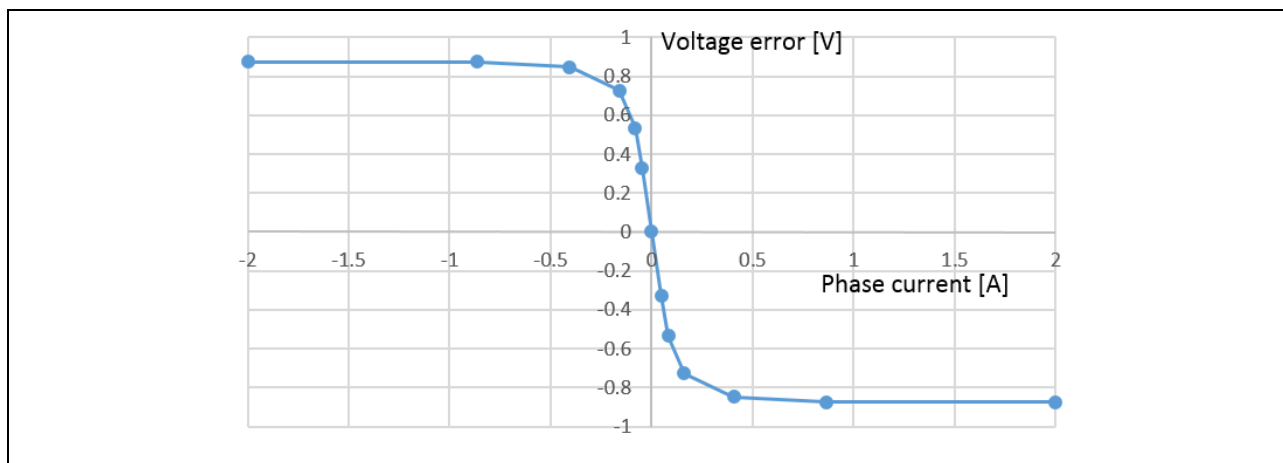
Figure 4-7 Current Dependence of Voltage Error (Example)

4.5   Pulse Width Modulation (PWM)

As a general implementation of the vector control for PMSMs, phase voltage references are generated as sine wave. However, when sin wave voltage reference is used as modulation wave for PWM generation, voltage utilization factor is limited by 86.7 [%]. To increase the voltage utilization factor, the modified three-phase voltage reference is used as modulation wave. The modified three-phase voltage reference (V_u', V_v', V_w') is calculated by subtracting average value of maximum and minimum from three-phase voltage (V_u, V_v, V_w). Then, without changing line-to-line voltage, the maximum amplitude of the modulation wave becomes $\sqrt{3}/2$ times, and as a result the voltage efficiency rate becomes 100[%].

$$\begin{pmatrix} V_u' \\ V_v' \\ V_w' \end{pmatrix} = \begin{pmatrix} V_u \\ V_v \\ V_w \end{pmatrix} + \Delta V \begin{pmatrix} 1 \\ 1 \\ 1 \end{pmatrix}$$

$$\because \Delta V = -\frac{V_{max} + V_{min}}{2} \ , \ V_{max} = max\{V_u, V_v, V_w\} \ , \ V_{min} = min\{V_u, V_v, V_w\}$$

V_u, V_v, V_w: U, V, W phase voltage reference

V_u', V_v', V_w': U, V, W phase voltage reference for PWM generation (Modulation wave)

4.6　Block Diagram of Sensorless Vector Control

Figure 4-8 shows block diagram sensorless vector control using BEMF observer when open-loop control is in use.
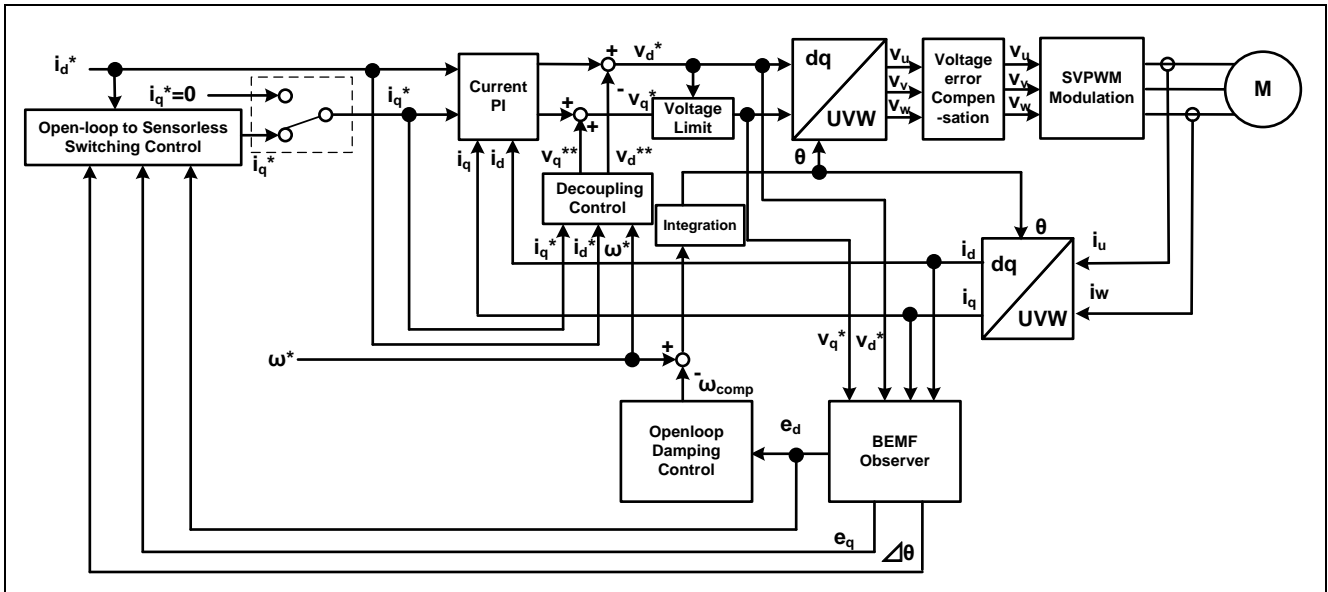
Figure 4-8 Block Diagram of Sensorless Vector Control (Open-Loop Control)

Figure 4-9 shows block diagram of sensorless vector control using BEMF observer when sensorless control (closed loop control) is in use.
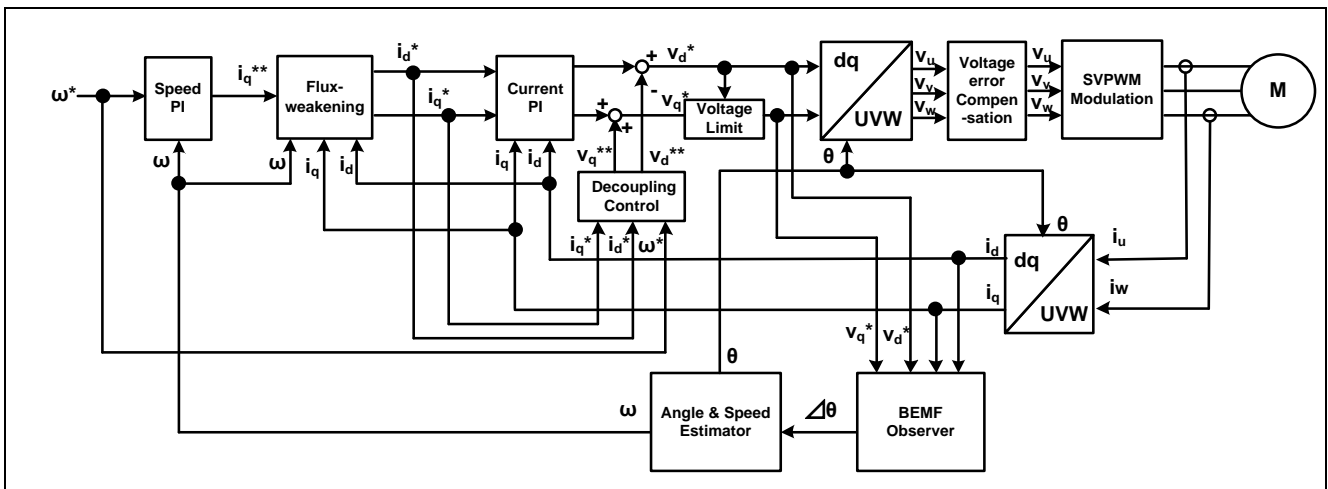
Figure 4-9 Block Diagram of Sensorless Vector Control (Sensorless Control)

4.7   Startup Sequence

Figure 4-10 shows the example of startup control of the sensorless vector control.
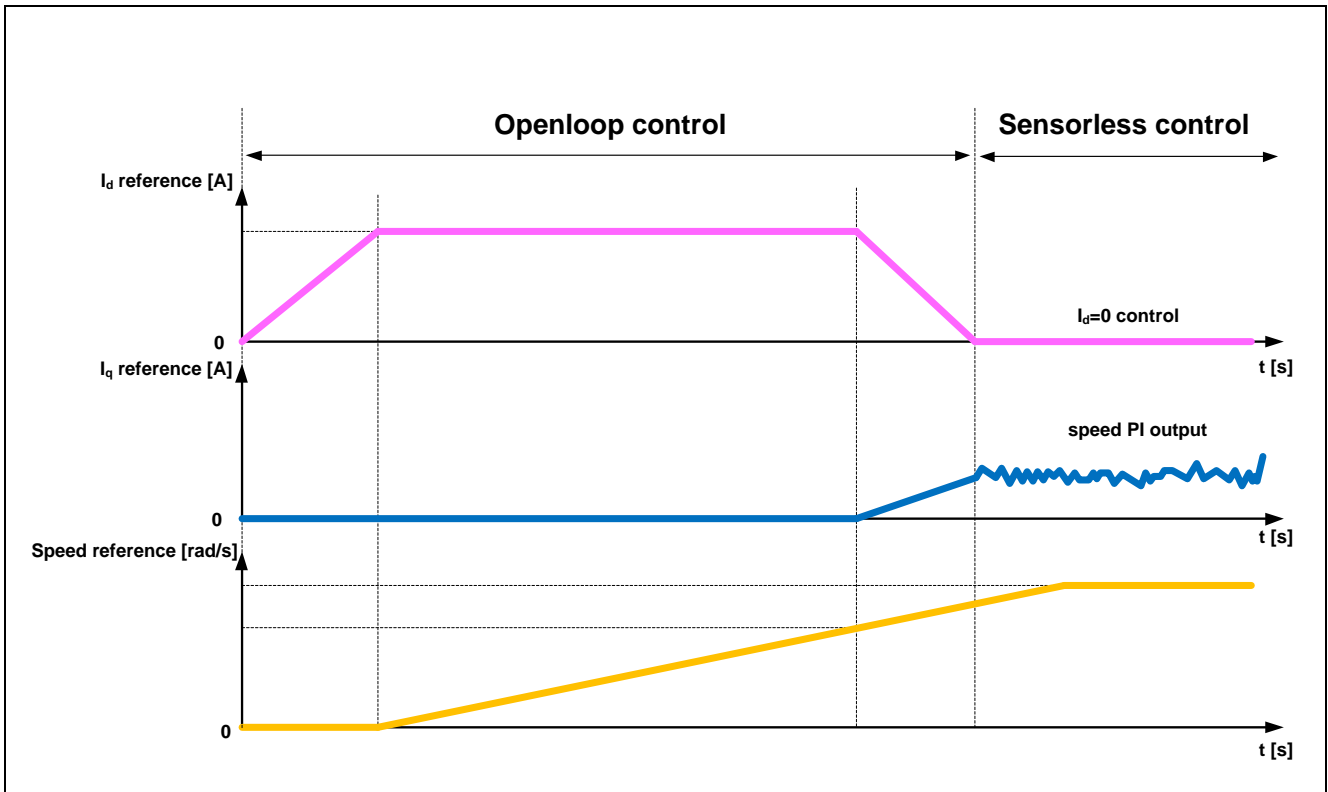
Figure 4-10 Startup Control of the Sensorless Vector Control (Example)

Website and Support

Renesas Electronics Website
http://www.renesas.com/

Inquiries
http://www.renesas.com/contact/

Revision History

			Description
Rev.	Date	Page	Summary
1.00	Apr. 05, 2017	-	First edition issued
1.01	Jul. 07,2017	-	Fixed typo error in document
1.02	Oct. 31,2018	-	Fixed typo error in document

General Precautions in the Handling of Microprocessing Unit and Microcontroller Unit Products

The following usage notes are applicable to all Microprocessing unit and Microcontroller unit products from Renesas. For detailed usage notes on the products covered by this document, refer to the relevant sections of the document as well as any technical updates that have been issued for the products.

1. Handling of Unused Pins

   Handle unused pins in accordance with the directions given under Handling of Unused Pins in the manual.

   — The input pins of CMOS products are generally in the high-impedance state. In operation with an unused pin in the open-circuit state, extra electromagnetic noise is induced in the vicinity of LSI, an associated shoot-through current flows internally, and malfunctions occur due to the false recognition of the pin state as an input signal become possible. Unused pins should be handled as described under Handling of Unused Pins in the manual.

2. Processing at Power-on

   The state of the product is undefined at the moment when power is supplied.

   — The states of internal circuits in the LSI are indeterminate and the states of register settings and pins are undefined at the moment when power is supplied.
   In a finished product where the reset signal is applied to the external reset pin, the states of pins are not guaranteed from the moment when power is supplied until the reset process is completed.
   In a similar way, the states of pins in a product that is reset by an on-chip power-on reset function are not guaranteed from the moment when power is supplied until the power reaches the level at which resetting has been specified.

3. Prohibition of Access to Reserved Addresses

   Access to reserved addresses is prohibited.

   — The reserved addresses are provided for the possible future expansion of functions. Do not access these addresses; the correct operation of LSI is not guaranteed if they are accessed.

4. Clock Signals

   After applying a reset, only release the reset line after the operating clock signal has become stable. When switching the clock signal during program execution, wait until the target clock signal has stabilized.

   — When the clock signal is generated with an external resonator (or from an external oscillator) during a reset, ensure that the reset line is only released after full stabilization of the clock signal. Moreover, when switching to a clock signal produced with an external resonator (or by an external oscillator) while program execution is in progress, wait until the target clock signal is stable.

5. Differences between Products

   Before changing from one product to another, i.e. to a product with a different part number, confirm that the change will not lead to problems.

   — The characteristics of Microprocessing unit or Microcontroller unit products in the same group but having a different part number may differ in terms of the internal memory capacity, layout pattern, and other factors, which can affect the ranges of electrical characteristics, such as characteristic values, operating margins, immunity to noise, and amount of radiated noise. When changing to a product with a different part number, implement a system-evaluation test for the given product.

RENESAS

Renesas Electronics Corporation

http://www.renesas.com